

# Distortion management in slow-light pulse delay

Michael D. Stenner and Mark A. Neifeld

University of Arizona, Department of Electrical and Computer Engineering and The Optical Sciences Center, Tucson, Arizona, 85721 USA

[mstenner@ece.arizona.edu](mailto:mstenner@ece.arizona.edu)

Zhaoming Zhu, Andrew M. C. Dawes, and Daniel J. Gauthier

Duke University, Department of Physics, and The Fitzpatrick Center for Photonics and Communications Systems, Durham, North Carolina, 27708 USA

**Abstract:** We describe a methodology to maximize slow-light pulse delay subject to a constraint on the allowable pulse distortion. We show that optimizing over a larger number of physical variables can increase the distortion-constrained delay. We demonstrate these concepts by comparing the optimum slow-light pulse delay achievable using a single Lorentzian gain line with that achievable using a pair of closely-spaced gain lines. We predict that distortion management using a gain doublet can provide approximately a factor of 2 increase in slow-light pulse delay as compared with the optimum single-line delay. Experimental results employing Brillouin gain in optical fiber confirm our theoretical predictions.

© 2005 Optical Society of America

**OCIS codes:** (060.5530) Pulse propagation and solitons; (290.5900) Scattering, stimulated Brillouin

---

## References and links

1. R. W. Boyd and D. J. Gauthier, "'Slow' and 'Fast' Light," in *Progress in Optics, Vol. 43*, E. Wolf, ed. (Elsevier, Amsterdam, 2002), pp. 497–530.
2. Y. A. Vlasov, S. Petit, G. Klein, B. Hönerlage, and C. Hirlimann, "Femtosecond measurements of the time of flight of photons in a three-dimensional photonic crystal," *Phys. Rev. E* **60**, 1030–1035 (1999).
3. J. E. Heebner, R. W. Boyd, and Q. Park, "Slow light, induced dispersion, enhanced nonlinearity, and optical solitons in a resonator-array waveguide," *Phys. Rev. E* **65**, 036619 (2002).
4. Y. Xu, R. K. Lee, and A. Yariv, "Scattering theory analysis of waveguide-resonator coupling," *Phys. Rev. E* **62**, 7389–7404 (2000).
5. A. Yariv, Y. Xu, R. K. Lee, and A. Scherer, "Coupled resonator optical waveguide: a proposal and analysis," *Opt. Lett.* **24**, 711–713 (1999).
6. R. W. Boyd, D. J. Gauthier, A. L. Gaeta, and A. E. Willner, "Maximum time delay achievable on propagation through a slow-light medium," *Phys. Rev. A* **71**, 023801 (2005).
7. H. Cao, A. Dogariu, and L. J. Wang, "Negative group delay and pulse compression in superluminal pulse propagation," *IEEE J. Sel. Top. Quantum Electron.* **9**, 52–58 (2003).
8. B. Macke and B. Ségard, "Propagation of light-pulses at a negative group-velocity," *European Phys. J. D* **23**, 125–141 (2003).
9. M. Bashkansky, G. Beadie, Z. Dutton, F. K. Fatemi, J. Reintjes, and M. Steiner, "Slow-light dynamics of large-bandwidth pulses in warm rubidium vapor," *Phys. Rev. A* **72**, 033819 (2005).
10. Y. Okawachi, M. S. Bigelow, J. E. Sharping, Z. M. Zhu, A. Schweinsberg, D. J. Gauthier, R. W. Boyd, and A. L. Gaeta, "Tunable all-optical delays via Brillouin slow light in an optical fiber," *Phys. Rev. Lett.* **94**, 153902 (2005).
11. K. Y. Song, M. G. Herráez, and L. Thévenaz, "Observation of pulse delaying and advancement in optical fibers using stimulated Brillouin scattering," *Opt. Express* **13**, 82–88 (2005) <http://www.opticsexpress.org/abstract.cfm?URI=OPEX-13-1-82>.

12. K. Y. Song, M. G. Herráez, and L. Thévenaz, "Long optically controlled delays in optical fibers," *Opt. Lett.* **30**, 1782–1784 (2005).
13. Z. Zhu, D.J. Gauthier, Y. Okawachi, J.E. Sharping, A.L. Gaeta, R.W. Boyd, and A.E. Willner, "Numerical study of all-optical slow-light delays via stimulated Brillouin scattering in an optical fiber," to appear in *J. Opt. Soc. Am. B* **22** (2005).
14. A. V. Oppenheim and A. S. Willsky, *Signals and Systems, 2nd Ed.* (Prentice Hall, Upper Saddle River, 1997).
15. Y. Chen, G. Pasrija, B. Farhang-Boroujeny, and S. Blair, "Engineering the nonlinear phase shift," *Opt. Lett.* **28** 1945–1947 (2003).
16. G. Lenz, B. J. Eggleton, C. K. Madsen, and R. E. Slusher, "Optical delay lines based on optical filters," *IEEE J. Quantum Electron.* **37** 525–532 (2001).
17. J. E. Heebner, P. Chak, S. Pereira, J. E. Sipe, R. W. Boyd, "Distributed and localized feedback in microresonator sequences for linear and nonlinear optics," *J. Opt. Soc. Am. B*, **21** 1818–1832 (2004).
18. M. Nikles, L. Thévenaz, and P. A. Robert, "Brillouin gain spectrum characterization in single-mode optical fibers," *J. Lightwave Technol.* **15**, 1842–1851 (1997).
19. Z. Dutton, M. Bashkansky, M. Steiner, and J. Reintjes, "Channelization architecture for wide-band slow light in atomic vapors," *SPIE* **5735**, 115–129 (2005).
20. Q. Sun, Y. V. Rostovtsev, J. P. Dowling, M. O. Scully, and M. S. Zhubairy, "Optically controlled delays for broadband pulses," *Phys. Rev. A* **72** 031802(R) (2005).

Over the last decade, there has been great progress in devising new methods for tailoring the dispersion of optical materials, such as electromagnetically induced transparency [1], photonic crystals [2], and nano-optic resonators [3–5]. This work has been motivated by the need for electronically or optically controllable pulse delays for applications such as optical buffers, data synchronization, optical memories, and signal processing. In these applications, the primary requirements for slow-light pulse delay are that the temporal pulse delay  $t_d$  be large relative to the pulse width  $\tau$  and that the pulse not be substantially distorted (defined below). These two requirements largely oppose each other, with large delay coming at the cost of greater distortion. These tradeoffs have been studied in simple Lorentzian systems [6–8] and in Doppler-broadened media [9] with encouraging results, but distortion remains a major limitation to the usefulness of slow-light pulse delay.

In this paper, we present a method for achieving large slow-light pulse delay under the constraint that the distortion does not exceed a particular limit. We also present a simple distortion-managed medium based on dual Lorentzian gain lines. The dispersive properties of this medium are tailored by adjusting the spacing between two adjacent gain lines. We predict nearly a factor of 2 improvement in the relative slow-light pulse delay for the two-gain-line case in comparison to the best single-gain-line case for the same distortion constraint in both cases. We demonstrate dispersion-managed pulse delay in an experiment where the slow-light effect arises from the dispersion associated with stimulated Brillouin scattering (SBS) resonances in a pumped optical fiber [10–13].

For pulses propagating through linear optical systems, the output pulse amplitude  $A(\omega, z)$  in the frequency domain can be related to the input pulse amplitude  $A(\omega, 0)$  by

$$A(\omega, z) = A(\omega, 0)e^{ik(\omega)z}, \quad (1)$$

where  $z$  is the length of the medium and  $k(\omega)$  is the complex wavenumber as a function of frequency  $\omega$ . A pulse propagates undistorted through a dispersive material when  $k(\omega)$  takes the form

$$k(\omega) = k_0 + k_1(\omega - \omega_c), \quad (2)$$

where  $\omega_c$  is the carrier frequency of the pulse and  $k_1$  is real. That is, the pulse shape remains unchanged and the only effects of propagation are delay, an overall phase shift, and gain or attenuation. In this ideal case, the pulse delay  $t_d$  is equal to the group delay  $t_g = z(k_1 - 1/c)$ , where  $c$  is the speed of light in vacuum. In practice, dispersive media do not satisfy Eq. (2)

precisely, but have higher-order terms in the Taylor expansion  $k(\omega) = \sum_{j=0}^{\infty} k_j(\omega - \omega_c)^j/j!$ , where  $k_j \equiv d^j k(\omega)/d\omega^j$ . These higher-order terms can lead to pulse distortion, or a change in the pulse shape. One can always use pulses with narrower bandwidth, and thereby improve the linearity of  $k(\omega)$  over the pulse bandwidth, but this results in longer pulses without increasing the delay. It is sometimes possible to simultaneously increase  $k_1$  and decrease the pulse bandwidth, which can result in larger relative delays, but may result in unacceptably large gain or absorption [6].

One method for creating delayed pulses with minimal distortion is to reduce the effects of the higher-order terms in the Taylor series expansion of  $k(\omega)$ . The effects of these terms have been studied in simple systems [6–9, 13], but additional degrees of freedom can be used to eliminate or balance them. We propose using custom slow-light media designed to minimize the effects of distortion. Creating a custom dispersion profile  $k(\omega)$  is in general quite difficult. However, one can instead create a custom system by combining multiple simple systems. We consider here a system composed of two Lorentzian gain lines; a gain doublet, as shown in Fig. 1. The wavenumber of such a system is given by

$$k(\omega) = \frac{\omega}{c}n_0 + \frac{g_0}{z} \left( \frac{\gamma}{\omega - (\omega_0 - \delta) + i\gamma} + \frac{\gamma}{\omega - (\omega_0 + \delta) + i\gamma} \right), \quad (3)$$

where  $n_0$  is the background refractive index,  $g_0/z$  is the line-center amplitude gain coefficient for each line,  $\gamma$  is the linewidth, and  $2\delta$  is the separation between the lines. In many slow-light media, the dominant source of distortion is the second-order term in the expansion of  $k(\omega)$ ,  $k_2$  [6]. For the gain doublet, we have

$$k_2 = -\frac{4ig_0\gamma^2}{z} \frac{3\delta^2 - \gamma^2}{(\delta^2 + \gamma^2)^3}. \quad (4)$$

As can be seen from Eq. (4),  $k_2 = 0$  for a separation of  $\delta = \gamma/\sqrt{3}$ , thereby eliminating the lowest-order distortion-causing term. For a doublet in this configuration, the group delay is given by

$$t_g = z(k_1 - 1/c) = \frac{z}{c}(n_0 - 1) + \frac{3}{4} \frac{g_0}{\gamma}, \quad (5)$$

which should be compared to the delay for a single line

$$t_g = \frac{z}{c}(n_0 - 1) + \frac{g_0}{\gamma}. \quad (6)$$

By comparing Eqs. (5) and (6), it is seen that the group delays for these two systems are very similar. While this result is interesting and illuminating, it is of limited practical value; it eliminates only second-order distortion, ignoring all higher-order terms.

A more practical approach to distortion management is to measure distortion as the deviation of the medium from the ideal one described in Eq. (2). At this point, it becomes convenient to describe the medium in terms of its transfer function  $H(\omega)$ , which is easily related to  $k(\omega)$  by  $H(\omega) = \exp(ik(\omega)z)$ . An ideal medium has a transfer function with constant amplitude  $|H(\omega)| = H_0$  and a phase that varies linearly with frequency  $\angle H(\omega) = t_p\omega$ , where  $t_p$  is the total propagation time of the pulse. Relating these to Eq. (2) yields  $H_0 = \exp[i(k_0 - k_1\omega_0)z]$  and  $t_p = k_1z$ . Any deviation from this behavior leads to pulse distortion [14].

There are many ways to quantify the deviation of the transfer function from ideal. One very simple way is to calculate the infinity-norm—the maximum magnitude—of the amplitude and phase deviation from ideal. This leads to two distortion metrics, one for the amplitude variation

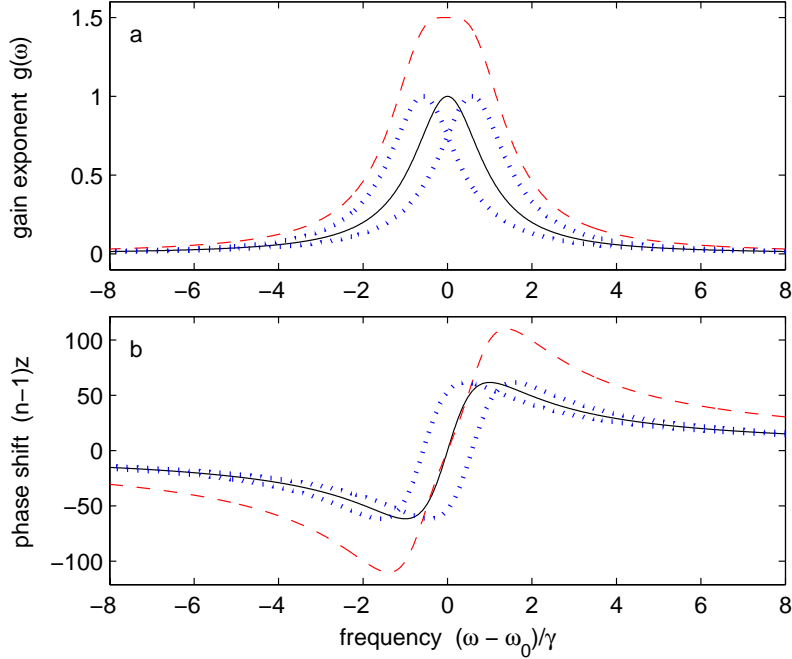


Fig. 1. Gain and dispersion for a single Lorentzian line (solid) and a doublet with separation  $\delta = \gamma/\sqrt{3}$  (dashed). Also shown are the two constituent lines (dotted) that make up the doublet. (a) The gain exponent has a broad flat top (a result of setting  $k_2 = 0$ ), although it is larger for the same value of the individual gain coefficients. (b) The central region of approximately linear dispersion is very similar for both systems near the center of the lines, but extends farther for the gain-doublet case.

( $D_a$ ) and one for the phase variation ( $D_p$ ). The amplitude distortion is given by

$$D_a = \frac{H_{\max} - H_{\min}}{H_{\max} + H_{\min}}, \quad (7)$$

where  $H_{\min}$  and  $H_{\max}$  are the minimum and maximum values of  $|H(\omega)|$  over the frequency range  $(\omega_0 - \Delta_b, \omega_0 + \Delta_b)$ . Similarly, we define the phase distortion as

$$D_p = \frac{1}{2\pi} \max_{\omega_0 - \Delta_b}^{\omega_0 + \Delta_b} [|\angle H(\omega) - (t_p \omega + \phi_0)|], \quad (8)$$

where  $t_p$  and  $\phi_0$  are chosen to minimize  $D_p$ . This provides a very conservative distortion measure for pulses whose power falls entirely within the frequency range  $(\omega_0 - \Delta_b, \omega_0 + \Delta_b)$ . The calculation of  $D_p$  also serves to define an effective propagation time  $t_p$  as the propagation time of a pulse through the ideal medium most closely approximated by the real medium. A delay defined in terms of this propagation time  $t_d = t_p - n_0 z/c$  is similar in concept to the group delay, except that it is based on the material dispersion over the entire bandwidth of interest rather than just at the carrier frequency. In fact, the pulse delay  $t_d$  is exactly equal to the group delay of the best-fit ideal medium. Because this delay includes dispersive effects over the entire bandwidth of interest, it provides a better prediction of actual pulse delay (peak delay, for example) than the group delay. As is common in communication systems [14], pulses with power extending outside this range can still be used, but the result is then approximate. These distortion metrics are reasonable in the case where the signal spectrum is approximately limited to the given

bandwidth window but is otherwise unknown. If more is known about the signal spectrum, then more complicated distortion measures can be used that consider a fixed spectrum and the form of the material deviation from ideal.

Having defined these distortion metrics, we can use them to explore the gain-doublet slow-light media discussed above. Let us first consider the simple Lorentzian gain line, whose transfer function can be written as

$$\begin{aligned} H_1(\omega) &= \exp\left(izn_0\frac{\omega}{c}\right) \times \exp(g_1(\omega)) \\ &= \exp\left(izn_0\frac{\omega}{c} + g_{01}\frac{i\gamma}{(\omega - \omega_0) + i\gamma}\right). \end{aligned} \quad (9)$$

Holding  $\gamma$  fixed, we find that for each  $\Delta_b$  there is an optimum value of  $g_{01}$  that provides maximum delay  $t_d$  subject to gain and distortion constraints. We have chosen to use an amplitude gain constraint of  $g_{01} \leq 2.5$  so that the system can be reasonably implemented experimentally. Larger gain is often accompanied by nonlinear optical effects.

The communication system of interest will define both the appropriate form of the relevant distortion and its maximum allowed value. In conjunction with the infinity norm, we select a conservative value of maximum allowed distortion  $D_a < 0.05$  and  $D_p < 0.05$ . This value is somewhat arbitrary and results in pulse distortion that is just noticeable upon visual inspection.

Figure 2(a) shows the maximum relative delay  $t_d\Delta_b$  as a function of the relative bandwidth  $\Delta_b/\gamma$ . Figure 2(b) shows the Lorentzian gain exponent  $g_{01}$ . At each value of  $\Delta_b$ , the gain is chosen to maximize the delay subject to the gain and distortion constraints described above. By comparing the solid lines in Figs. 2(a) and 2(b), we observe two bandwidth regions, separated by a cusp. We see that the delay is limited by the distortion constraint for large relative bandwidths— $\Delta_b/\gamma > 0.2$ ; driving the gain higher will produce too much distortion. For small bandwidths, the delay is limited by the gain constraint. The maximum relative delay is achieved at some intermediate bandwidth— $\Delta_b/\gamma \approx 0.2$ —for which both distortion and gain limits are met simultaneously. At this value, we find a maximum relative delay of  $t_d\Delta_b \approx 0.5$  under the constraint that neither  $D_a$  nor  $D_p$  exceed 0.05.

We now consider a distortion-managed system constructed using two nearby Lorentzian gain lines in a manner that is analogous to multi-stage filter design [15–17]. The transfer function of this system is

$$\begin{aligned} H_2(\omega) &= \exp\left(izn_0\frac{\omega}{c}\right) \times \exp(g_2(\omega)) \\ &= \exp\left(izn_0\frac{\omega}{c} + g_{02}\frac{i\gamma}{(\omega - \omega_0 - \delta) + i\gamma} + g_{02}\frac{i\gamma}{(\omega - \omega_0 + \delta) + i\gamma}\right). \end{aligned} \quad (10)$$

As above, we can optimize over the free parameters—now  $g_{02}$  and  $\delta$ —to maximize the delay at each  $\Delta_b$  subject to the same constraints,  $D_a \leq 0.05$ ,  $D_p \leq 0.05$ , and  $\max[|g_2(\omega)|] \leq 2.5$ . The dashed line in Fig. 2(a) shows distortion- and gain-limited relative delay as a function of bandwidth for this doublet system.

As described above, the second order distortion—dominant in many low-distortion cases—can be eliminated entirely ( $k_2 = 0$ ) by setting  $\delta = \gamma/\sqrt{3} \rightarrow \delta/\gamma \approx 0.58$ . One might expect this result to provide the optimal line separation. However, as shown in Fig. 2(c), delay can be increased at large bandwidths by using a larger separation because, although there is a gain dip at the carrier frequency, the gain excursion over the full bandwidth can be minimized. For small bandwidths, a smaller separation is desirable because the delay is limited by gain, not distortion, and so it is more useful to make the separation small, creating larger dispersion for the same maximum gain.

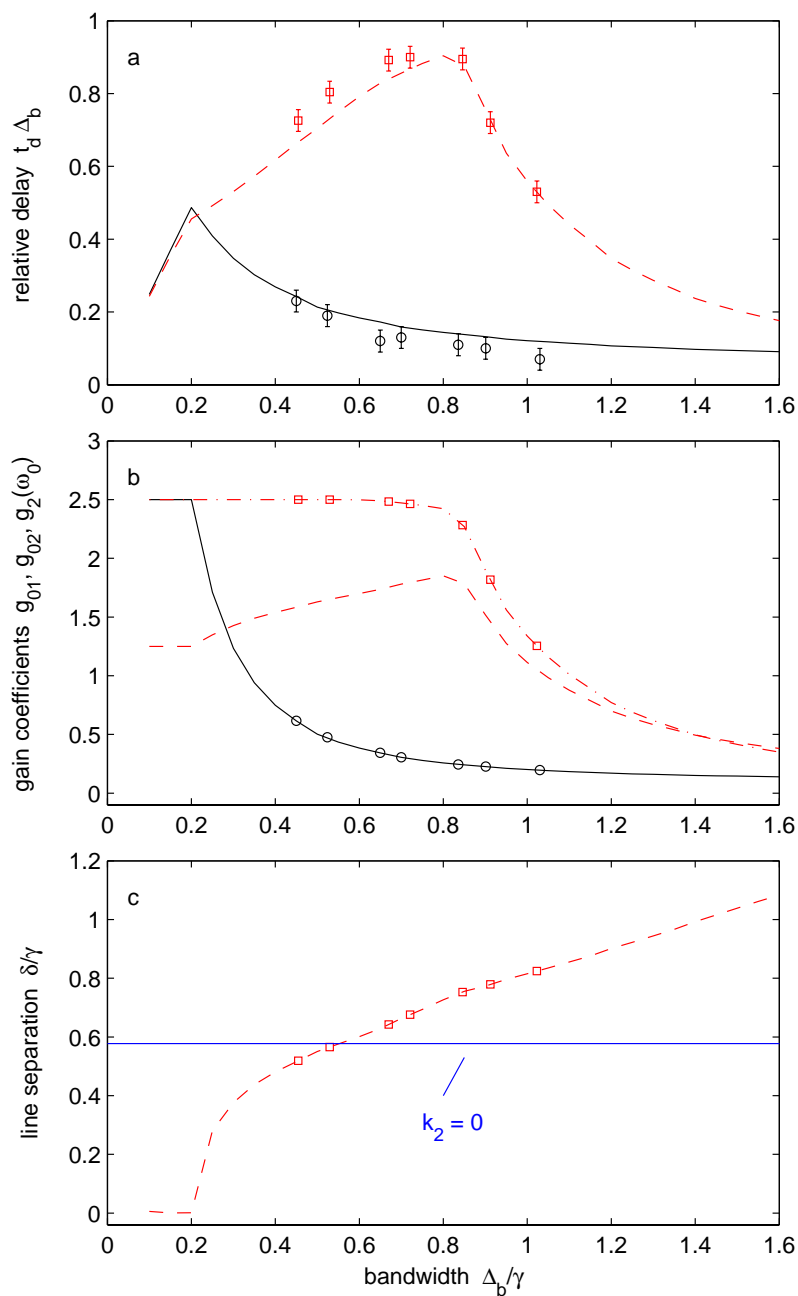


Fig. 2. Simulation and experimental results for both the single Lorentzian line (solid lines for simulation, circles for experimental results) and the doublet (dashed lines for simulation, squares for experimental results). (a) Relative delay. (b) Lorentzian line-center amplitude gain coefficients  $g_{01}$  and  $g_{02}$ . Also shown is the center-frequency gain coefficient for the doublet  $g_2(\omega_0)$  (dot-dashed). (c) Line separation for the doublet. The horizontal line indicates the value of  $\delta/\gamma$  that leads to  $k_2 = 0$

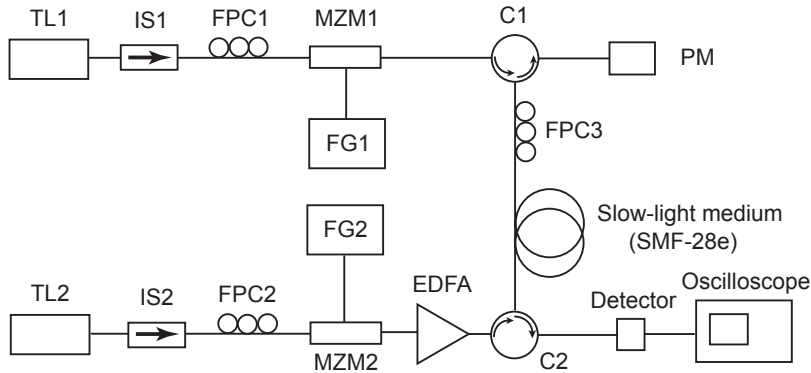


Fig. 3. Experiment setup based on a fiber Brillouin amplifier. TL1, TL2: tunable lasers; IS1, IS2: isolators; FPC1, FPC2, FPC3: fiber polarization controllers; MZM1, MZM2: Mach-Zehnder modulators; FG1, FG2: function generators; EDFA: Erbium-doped fiber amplifier; C1, C2: circulators; SMF-28e: 500-m-long SMF-28e fiber (the SBS amplifier); PM: power meter.

There are three distinct frequency regions on these plots separated by two obvious cusps. The left-most region ( $\Delta_b/\gamma < 0.25$ ) corresponds to gain-limited configurations where in which the distortion is not reached, and so the second line provides no additional benefit. The right-most region ( $\Delta_b/\gamma > 0.8$ ) corresponds to the distortion-limited regime where the maximum gain cannot be reached. In the central region, both distortion and gain constraints are hit simultaneously. In this gain-doublet medium, we observe a maximum relative delay of 0.9 at a bandwidth of  $\Delta_b/\gamma = 0.8$ , an improvement by a factor of 6.25 over the single line at that bandwidth and nearly twice the best single-line relative delay.

To test our distortion-management concept, we propagate optical pulses through a SBS slow-light medium [10–13]. A gain-doublet with an adjustable frequency separation  $2\delta$  is realized by pumping a standard room-temperature telecommunications optical fiber with a bichromatic laser field, which is obtained via carrier-frequency-suppression modulation of a continuous-wave (CW) single-frequency laser field [18]. The doublet spacing  $2\delta$  is adjusted by changing the frequency of the voltage driving the modulator and the gain coefficient (and hence the slow-light delay) is adjusted by changing the pump power. Either of these adjustments can be made very quickly, limited by the transit time of the pump field through the optical fiber.

The transfer function  $H_2(\omega)$  (Eq. (10)) can be realized by setting the carrier frequency of the pulses close to the SBS amplifying resonances (the so-called Stokes resonances) and keeping the pulse intensity low enough so that the response is linear. For comparison, we also propagate pulses through a standard slow-light medium with a single gain resonance, corresponding to  $H_1(\omega)$  (Eq. (9)) and realized using a single-frequency pump field [10–13].

The experimental setup is shown schematically in Fig. 3. Two 1550-nm narrow-linewidth tunable lasers (TL1 and TL2) are used to produce Stokes signal pulses and the pump beams, respectively. A bichromatic pump beam is produced by passing the single-frequency CW laser beam generated by TL2 (angular frequency  $\omega_p$ ) through modulator MZM2, which is driven by a sinusoidal voltage of angular frequency  $\delta$ . The bias voltage applied to MZM2 is chosen to suppress the carrier frequency, resulting in a beam with frequencies  $(\omega_p \pm \delta)$ . This beam is amplified by an erbium-doped fiber amplifier (EDFA) and routed via circulator C2 to pump a 500-m-long SMF-28e fiber (the slow-light medium). For this fiber, we measure an SBS linewidth (full-width at half-maximum) of  $\gamma/\pi \simeq 35$  MHz. After passing through the slow-light medium, the beam is routed out of the system via circulator C1 and monitored by a power meter.

The signal pulses are produced from a laser beam generated by TL1. The beam passes through an isolator, a fiber polarization controller, and modulator MZM1, producing pulses with carrier frequency  $\omega_c$ . They are approximately Gaussian-shaped with an intensity envelope of the form  $I(t) = I_0 \exp[-(t/\tau)^2]$ , where the spectrum  $S(\omega) \propto \exp[-\tau^2(\omega - \omega_c)^2]$  has a  $1/e$  half width of  $\Delta_0 = 1/\tau$ . The pulses enter the 500-m-long SMF-28e fiber via circulator C1 and counterpropagate with respect to the bichromatic pump beam in the fiber. The slow-light-delayed and amplified pulses are routed out of the system via C2, sensed by a fast photodetector, and displayed on a digital oscilloscope. The frequency difference between TL1 and TL2 is tuned so that the pulse carrier frequency is set precisely to the center of the SBS amplifying resonances,  $\omega_c = \omega_0$  where  $\omega_0 = \omega_p - \Omega_B$ , and  $\Omega_B/2\pi = 12.5$  GHz is the Brillouin frequency shift for the SMF-28e fiber. Fiber polarization controllers FPC1 and FPC2 are used to maximize the transmissions through the Mach-Zehnder modulators, and FPC3 is used to maximize the SBS slow-light delay experienced by the Stokes pulses.

In the experiments with the distortion-managed slow-light medium, we select a pulse bandwidth  $\Delta_b$  (using the assumption that  $\Delta_b = \Delta_0$ ), set the resonance half-separation  $\delta$  according to Fig. 2(c), set the central gain  $g_2(\omega_0)$  according to Fig. 2(b) by adjusting the pump power, and measure the delay of the peak of the pulses induced by the slow-light medium (which is approximately equal to  $t_d$ ). From Fig. 2(a), it is seen that the agreement with the theoretical predictions is very good. Also shown in Fig. 2(a) are our observations for a single-gain line (the non-distortion-managed slow-light medium), where the agreement between the observations and the predictions is excellent.

The data shown in Fig. 2(a) demonstrate that the distortion-managed slow-light medium vastly outperforms the standard slow-light medium under conditions of constant distortion. Around the optimum normalized bandwidth of  $\sim 0.84$  ( $\tau \sim 11$  ns), we measure an improvement in relative pulse delay of a factor of  $8.1 \pm 2.6$ . Thus, the distortion-managed approach substantially increases the usable bandwidth of a slow-light medium that is much easier to implement in comparison to previously suggested methods [19, 20].

In conclusion, we have shown that, although distortion limits the slow-light delay achievable in simple systems [6–8], it is possible to achieve better distortion- and gain-limited delay using custom composite media. Dramatic improvement can be achieved over a single Lorentzian line with a system as simple as a Lorentzian doublet, suggesting that even greater improvement may be achievable using more flexible media.

We gratefully acknowledge the financial support of the DARPA DSO Slow-Light Program and AFOSR contract #F49620-01-10363.